

# Effect of a built-in electric field in asymmetric ferroelectric tunnel junctions

Yang Liu,<sup>1,2,\*</sup> Xiaojie Lou,<sup>1</sup> Manuel Bibes,<sup>3</sup> and Brahim Dkhil<sup>2</sup>

<sup>1</sup>*Multi-disciplinary Materials Research Center, Frontier Institute of Science and Technology, Xi'an Jiaotong University, Xi'an 710054, People's Republic of China*

<sup>2</sup>*Laboratoire Structures, Propriétés et Modélisation des Solides, UMR 8580 CNRS-Ecole Centrale Paris, Grande Voie des Vignes, 92295 Châtenay-Malabry Cedex, France*

<sup>3</sup>*Unité Mixte de Physique CNRS/Thales, 1 Av. A. Fresnel, Campus de l'Ecole Polytechnique, 91767 Palaiseau and Université Paris-Sud, 91405 Orsay, France*

The contribution of a built-in electric field to ferroelectric phase transition in asymmetric ferroelectric tunnel junctions is studied using a multiscale thermodynamic model. It is demonstrated in details that there exists a critical thickness at which an unusual ferroelectric-“polar non-ferroelectric” phase transition occurs in asymmetric ferroelectric tunnel junctions. In the “polar non-ferroelectric” phase, there is only one non-switchable polarization which is caused by the competition between the depolarizing field and the built-in field, and closure-like domains are proposed to form to minimize the system energy. The transition temperature is found to decrease monotonically as the ferroelectric barrier thickness is decreased and the reduction becomes more significant for the thinner ferroelectric layers. As a matter of fact, the built-in electric field does not only result in smearing of phase transition but also forces the transition to take place at a reduced temperature. Such findings may impose a fundamental limit on the work temperature and thus should be further taken into account in the future ferroelectric tunnel junction-type or ferroelectric capacitor-type devices.

## INTRODUCTION

Ferroelectric (FE) tunnel junctions (FTJs) that are composed of FE thin films of a few unit cells sandwiched between two electrodes (in most cases the top and bottom electrodes are different) have attracted much more attention during the last decade. [1–3] It is generally believed that the interplay between ferroelectricity and quantum-mechanical tunneling plays a key role in determining tunnel electroresistance (TER) or tunneling current and TER effect usually takes place upon polarization reversal. Due to the strong coupling of FE polarization and the applied field, the electric-field control of TER or tunneling current, [1–11] spin polarization, [12–26] and electrocaloric effect [27] can be achieved, which makes FEs promising candidates for nondestructive FE storage, [1–10] FE memristor, [11] spintronics (magnetization), [12–26] or electrocaloric [27] devices. Meanwhile, another mechanically (including strain or strain gradient) induced TER is found recently, which also shows their potential applications in mechanical sensors, transducers and low-energy archive data storage devices. [28] Note that having different electrodes for the FTJs (some experiments use conductive atomic force microscope tips instead of the top electrodes) is usually required for a large effect at low bias voltage though the FTJs with same electrodes may also display interesting performances. [2, 4, 9, 18] Also note that all the functionalities in these devices are strongly related to the thermodynamic stability and switching ability of FTJs. [1–28] Therefore, a fundamental understanding of ferroelectricity of FTJs, especially their size effects, is crucial at the current stage of research.

Unfortunately, no consensus has been achieved on

whether there exists a critical thickness  $h_c$  below which the ferroelectricity disappears in FTJs, especially for those with different top/bottom electrodes. It is believed that an electrostatic depolarizing field caused by dipoles at the FE-metal interfaces is responsible for the size effect. [29–34] However, recent theoretical studies suggest that the choice of electrode material may lead to smearing of size effect or even vanishing of  $h_c$ . [35–39] For example, it was reported that choosing Pt as electrodes would induce a strong interfacial enhancement of the ferroelectricity in Pt/BaTiO<sub>3</sub>(BTO)/Pt FTJs, where  $h_c$  is only 0.08 BTO unit cell. [35] In addition, the results of a modified thermodynamic model [36, 37] and first-principles calculations [38, 39] both indicate that BTO barrier with dissimilar electrodes, i.e. Pt and SrRuO<sub>3</sub> (SRO) electrodes, might be free of deleterious size effects. In contrast, it has been reported that asymmetric combination of the electrodes (including the same electrodes with different terminations) will result in the destabilization of one polarization state making the asymmetric FTJs non-FE. [33, 40] And the up-to-date studies reported that the fixed interface dipoles near the FE/electrode interface is considered the main reason for that detrimental effect. [41, 42] Considering the importance of the physics in FTJs with dissimilar top and bottom electrodes, we are strongly motivated to investigate the size effect in such asymmetric FTJs.

It was pointed out as early as 1963 that the contribution of different electronic and chemical environments of the asymmetric electrode/FE interfaces would induce a large long-range electrostatic built-in electric field  $\vec{E}_{bi}$  in FE thin films. [43]  $\vec{E}_{bi}$  becomes more significant in asymmetric FTJs and should be taken into account. [33, 34] In this study, we use a multiscale ther-

modynamic model [27, 33, 34] to investigate the effect of such built-in electric field on the phase transition of asymmetric FTJs by neglecting the short-range interface dipoles. As a result, we discover an unusual FE-“polar non-FE” phase transition in asymmetric FTJs. Then, we make detailed analysis of the contribution of the built-in electric field to FE phase transition, i.e.  $h_c$ , what happens below  $h_c$ , transition temperature  $T_c$ , and temperature dependence of dielectric response of the asymmetric FTJs.

### MULTISCALE THERMODYNAMIC MODEL FOR THE FTJS

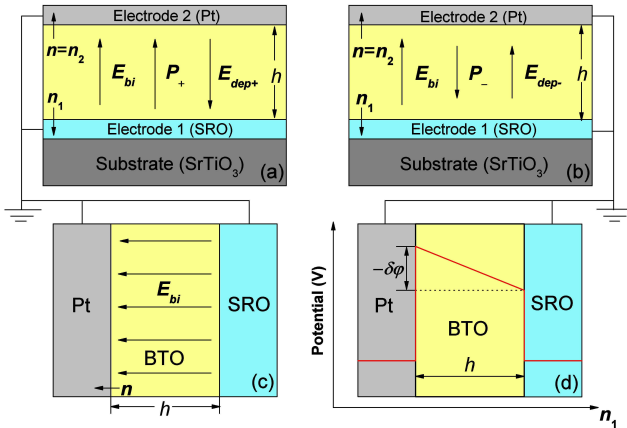


FIG. 1. Schematic configurations of the system considered in the present calculations for the asymmetric FTJs:  $P_+$  state (a);  $P_-$  state (b);  $\vec{E}_{bi}$  (c) and the corresponding potential profile at zero polarization (red line) (d).

We concentrate on a short-circuited (001) single-domain FE plate of thickness  $h$  sandwiched between different electrodes. The FE films are fully strained and grown on thick (001) substrate with the polar axis lying normal to the FE-electrode interfaces. [32–34] We denote the two interfaces as 1 and 2, with surface normals  $\vec{n}_1$  and  $\vec{n}_2 = -\vec{n}_1$  pointing into the electrodes. The configurations are schematically shown in Fig. 1. The exact value and direction of  $\vec{E}_{bi}$  can be determined as [33, 34]

$$\vec{E}_{bi} = -\frac{\Delta\varphi_2 - \Delta\varphi_1}{h}\vec{n} = -\frac{\delta\varphi}{h}\vec{n} \text{ and } \vec{n} = \vec{n}_2 = -\vec{n}_1, (1)$$

where  $\Delta\varphi_i$  which is the work function steps for FE-electrode  $i$  interface at zero polarization is simply defined as the potential difference between the FE and the electrode  $i$ . [33, 34] With the help of first-principles calculations, one could easily obtain  $\Delta\varphi_i$  through the analysis of the electrostatic potential of FTJs where FE films are in the paraelectric (PE) state. [33, 34]

Then, the free energy per unit surface of the FE layer is presented as [33, 34]

$$F = h\Phi + \Phi_S = \left(\frac{1}{2}\alpha_1^*P^2 + \frac{1}{4}\alpha_{11}^*P^4 + \frac{1}{6}\alpha_{111}P^6 + \frac{1}{8}\alpha_{1111}P^8 + \frac{u_m^2}{S_{11} + S_{12}} - \frac{1}{2}\vec{E}_{dep} \cdot \vec{P} - \vec{E}_{bi} \cdot \vec{P} - \vec{E} \cdot \vec{P}\right)h + (\zeta_1 - \zeta_2)\vec{n} \cdot \vec{P} + \frac{1}{2}(\eta_1 + \eta_2)P^2, \quad (2)$$

where  $\alpha_i^*$  are Landau coefficients. [27]  $u_m$  is the epitaxial strain and  $S_{mn}$  are the elastic compliances coefficients.  $\zeta_i$  and  $\eta_i$  are the first order and second order coefficients of the surface energy  $\Phi_S$  expansion for the two FE-electrode interfaces. [33, 34]  $\vec{E}$  is the applied electric field along the polar axis.  $\vec{E}_{dep}$  is the depolarizing field which can be determined from the short-circuit condition such that: [33, 34]

$$\vec{E}_{dep} = -\frac{\lambda_1 + \lambda_2}{h\varepsilon_0 + (\lambda_1 + \lambda_2)\varepsilon_b}\vec{P}, \quad (3)$$

where  $\varepsilon_0$  is the permittivity of vacuum space, and  $\varepsilon_b$  indicates the background (i.e. without contribution of the spontaneous polarization) dielectric constant.  $\lambda_i$  are the effective screening lengths of the two interfaces and are dependent on the polarization direction if the electronic and chemical environments of FE/electrode interfaces are different. [33, 34] For the two opposite polarization orientations, the direction dependence of  $\lambda_i$  will induce the asymmetry in potential energy and hence will produce the TER effect, besides the depolarizing field effect due to the polarization difference between two opposite orientations. [1–3] However, we ignore such an effect due to the lack of information about the direction dependence of  $\lambda_i$  and we mainly focus on the role of the built-in field in this study. Note that  $\delta\varphi$  and  $\delta\zeta = (\zeta_2 - \zeta_1)$  are thickness and polarization independent and  $\vec{E}_{bi}$  is indeed a long-range internal-bias field which has the effect of poling the FE film. [33, 34, 43] In asymmetric FTJs, such asymmetry parameters  $\delta\varphi$  and  $\delta\zeta$  can introduce a potential energy profile difference and therefore induce the TER effect. [1–3]

The equilibrium polarization can be derived from the condition of thermodynamic equilibrium:

$$\frac{\partial F}{\partial P} = 0. \quad (4)$$

The dielectric constant  $\varepsilon$  under an applied field  $E$  whose direction is along the polar axis can be determined as: [37]

$$\varepsilon = \frac{1}{h\varepsilon_0} \left( \frac{\partial^2 F}{\partial^2 P} \right)^{-1}. \quad (5)$$

The multiscale thermodynamic model used in this study combines first-principles calculations and phenomenological theory and its detailed description can

be found elsewhere. [33, 34] In the previous study, it is reported that  $\vec{E}_{bi}$  could result in a smearing of the phase transition and an internal-bias-induced piezoelectric response above  $T_c$  in asymmetric FTJs. [33] However, adding to the forgoing controversy on the size effects, further analysis of the effect of built-in field on the FE transition in asymmetric FTJs is still absent. Inserting Eq. (1) into Eq. (2) results in a term that encompasses an odd power of the polarization:  $\vec{E}_{bi} \cdot \vec{P}$ , which leads to asymmetric thermodynamic potentials. We shall show that this term which behaves mathematically as identically as the phenomenological term suggested by Bratkovsky and Levanyuk [44] will result in an unusual FE-“polar non-FE” phase transition in asymmetric FTJs.

## RESULTS AND DISCUSSION

### Size effects

For a quantitative analysis, we consider a fully strained BTO film sandwiched between Pt (electrode 2) and SRO (electrode 1) epitaxially grown on (001) SrTiO<sub>3</sub> substrates. We neglect the energy difference of the asymmetric surfaces, i.e. by setting  $\zeta_1 = \zeta_2$ ,  $\eta_1 = \eta_2$ , to insure that the effect of  $\vec{E}_{bi}$  is clearly observable from the calculations since it is reported that surface effects are generally much smaller than that of  $\vec{E}_{bi}$ . [36, 37] All the parameters we used are listed in Ref. 65. We first examine the effect of  $\vec{E}_{bi}$  on the ferroelectricity of asymmetric FTJs. Previous studies indicate that the direction of  $\vec{E}_{bi}$  in asymmetric Pt/BTO/SRO FTJs points to Pt electrode with higher work function. [36–38] All recent results show indeed that a strong preference for one polarization state namely  $P_+$  while  $P_-$  disappears at “ $h_c$ ”. [36–42] According to the definition of ferroelectricity, the spontaneous polarization of the FE materials is switchable under an ac electric field. [45] However, knowing that the spontaneous polarization of FE materials is switchable under an ac electric field, [45] recent reports [36–39] are rather confusing and remain incomplete on this point. Indeed, in addition to the forementioned divergence in the size effects, two different transition temperatures at which the two polarization states reach zero are obtained (see Ref. 37), which may be confusing since there should be only one finite phase transition temperature for disappearance of ferroelectricity. In order to avoid such confusions, we used the classical definition of ferroelectricity [45] in the following parts.

We make further analysis of the physical formulation of  $h_c$  in asymmetric FTJs. Note that Eq. (4) is a non-linear equation and yields “at most” three solutions  $P$ , two of them corresponding to minima and the other one to a saddle point (unstable state). Whether the solution is a minimum, a maximum or a saddle point can be revealed through inspecting the eigenvalues of the Hessian

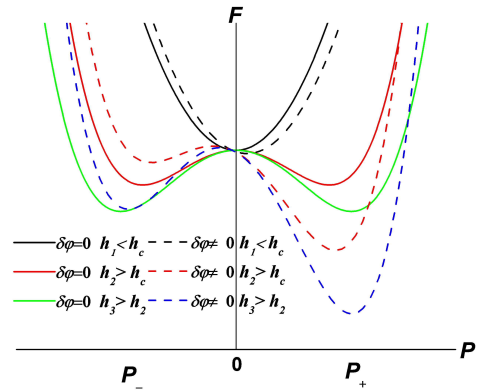


FIG. 2. Schematic representation of the variation in total free energy with respect to polarization with different BTO barrier thicknesses in asymmetric Pt/BTO/SRO tunnel junctions with/without consideration of the built-in field in zero applied field.

matrix of the total free energy  $F$ . Because the asymmetric FTJ is internally biased, i.e., the energy degeneracy between positive  $P_+$  and negative  $P_-$  is lifted, one of the minima corresponds to the equilibrium state (the global minimum) of the system (the direction of which is along  $\vec{E}_{bi}$ ) and the other minima corresponds to a metastable state (a local minimum) of the system. It means that the presence of two different electrodes in asymmetric FTJs results in a preferred polarization orientation of the FE plate. Having found all  $P$  solutions as a function of  $h$ , one can clearly see that metastable state and unstable state solutions become closer to each other and coincide at finite  $h$ , henceforth the number of solutions  $P$  drops from three to one. According to the bistable property of FE materials, this finite  $h$  is just  $h_c$ . [45] As long as there are three  $P$  solutions: two of these three solutions correspond to stable/metastable polarizations so that two orientations of polarization are possible in the BTO layer and thus it is FE. Switching the asymmetric FTJ into its unfavoured high energy polarization may be difficult. If there is the only  $P$  solution corresponding to the unstable state, although it attains a finite value, it is not FE anymore and may be called “PE”. Indeed it would be more appropriate to consider it as “polar non-FE” since  $P$  has a unique finite value. [46–48] FTJs with no built-in field  $\delta\varphi = 0$  will exhibit two energetically equivalent stable polarization states ( $P_+$  and  $P_-$ ) along with an unstable polarization state at  $P = 0$  below  $h_c$ . All the forgoing discussions can be clearly and easily understood in the schematic representation of  $F - P$  curves with different BTO thicknesses as shown in Fig. 2 which is quite similar with the results of FE thin films with/without consideration of the fixed interface dipoles near the asymmetric FE/electrode interface [40–

42] or FE superlattices with/without interfacial space charges. [48] Together with previous results, [41, 42] we conclude that no matter the  $\vec{E}_{bi}$  is considered as a long-range field or a short-range surface one, it cannot induce the vanishing of  $h_c$  in asymmetric FTJs, which is in contrast with other works. [36–39]

Note that “polar non-FE” phase is actually a pyroelectric phase because there is a non-switchable polarization in this phase. This kind of phase transition has once been reported in FE thin films with asymmetric electrodes [33, 40–42] or FE superlattices with interfacial space charge. [46–48] As we discussed in the formation of  $h_c$ , “polar non-FE” phase indeed always corresponds to the unstable state (see Fig. 2) and this kind of non-switchable polarization may not be stable at all. However, breaking up the system into  $180^\circ$  domain stripes is unambiguously ruled out due to the long-range pinned field  $\vec{E}_{bi}$ . In plane vortex formation [50, 51] is also inhibited because the large compressive strain favors more  $180^\circ$  domain stripes. [51] The ferromagneticlike closure domains are predicted to form in ultrathin FE films or FE capacitors even below  $h_c$  [52–54] and are experimentally confirmed well above  $h_c$  recently. [55, 56] However, typical FE closure domains [52–56] are also not expected in “polar non-FE” phase where  $180^\circ$  domains in the closure domain structure should be suppressed. But local rotations of non-switchable polarization ( $<90^\circ$ ) are still likely to occur and result in a closure-like domain structure since the local change of the direction of the non-switchable polarization especially near the FE/electrode interface is helpful to minimize the system energy. [52–54] Although such closure-like domains can be favored below  $h_c$  ( $<3$  nm at least), it is clear that the FE barrier as a whole is not FE according to our forgoing analysis that shows the polarization is not switchable under external electric fields. While a detailed analysis of the built-in field effect on domain formation is beyond the scope of this study, we suggest that more rigorous simulations should be made in the future. It can be seen that the asymmetric FTJs below  $h_c$  cannot be used for FE memory applications in which two thermodynamic stable polarization states are needed to encode “0” and “1” in Boolean algebra. [29–34, 45] However based on our calculation, one should expect a resistance change below  $h_c$  between the non-switchable polarization state and the other one being ferroelectrically dead. This result agrees well with recent works on Pt/BTO/Pt FTJs that even below  $h_c$ , the resistance of the FTJ would change by a factor of three due to the interface bonding and barrier decay rate effects. [4] We argue that the TER effect below  $h_c$  suggested in our work may be essentially attributed to the asymmetric modification of the potential barrier by the nonzero barrier height ( $-\delta\varphi$ ) (see Eqs. (1)–(4)) which even exists at zero polarization as shown in Fig. 1(d). Further theoretical and experimental efforts should be

made to confirm these predictions.

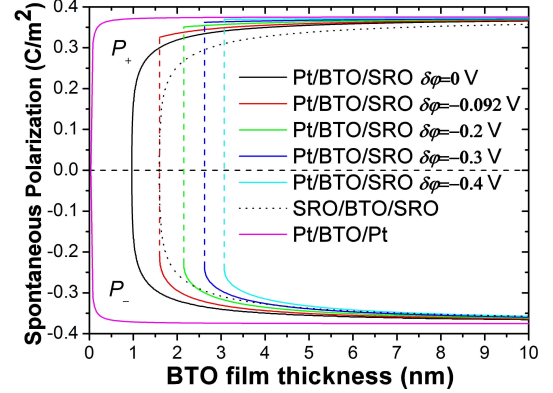


FIG. 3. Spontaneous polarization of the asymmetric Pt/BTO/SRO tunnel junctions as a function of BTO layer thickness with  $\delta\varphi=0$  V,  $-0.092$  V,  $-0.2$  V,  $-0.3$  V and  $0.4$  V in zero applied field at 0 K, respectively. The results of symmetric SRO/BTO/SRO and Pt/BTO/Pt tunnel junctions at 0 K [27] are also added for comparison.

The quantitative results of the forgoing analysis are directly given in Fig. 3. It can be seen that  $h_c$  exists regardless of symmetric or asymmetric structures. As expected, the curves of  $P_+$  and  $P_-$  are symmetric with respect to  $P = 0$  at  $\delta\varphi = 0$  where  $h_c$  is about 1 nm which is smaller than that of SRO/BTO/SRO, i.e. 1.6 nm. [27, 35] When  $\delta\varphi \neq 0$ , the supposed degeneracy between  $P_+$  and  $P_-$  occurs, i.e.  $P_+$  is enhanced while  $P_-$  is reduced so the coordinate of the center of the hysteresis loop along the polarization axis  $[1/2(P_+ + P_-)]$  is shifted along the direction of  $P_+$ . It is shown that such a displacement of the hysteresis loop along the polarization axis becomes more significant as the strength of  $\vec{E}_{bi}$  increases. It may be attributed to the imprint caused by  $\vec{E}_{bi}$  such that the whole shape of the hysteresis loop will shift along the direction of the field axis which is antiparallel to the direction of  $\vec{E}_{bi}$ . [45] Besides, it is found that as  $\delta\varphi$  increases,  $h_c$  increases, which indicates that  $\vec{E}_{bi}$  can enhance the size of  $h_c$ . Thus, whether  $h_c$  of Pt/BTO/SRO junction is larger or smaller than that in the SRO/BTO/SRO counterpart strongly depends on exact value of  $\delta\varphi$  as shown in Fig. 3.

For the symmetric structures (SRO/BTO/SRO and Pt/BTO/Pt FTJs), one can easily see in Fig. 3 that single domain in the FE layer destabilizes as the film thickness is decreased due to the depolarizing field effect. [27, 29–34] And it is shown in Fig. 3 that Pt/BTO/Pt FTJ whose  $h_c$  is merely 0.08 BTO unit cell is nearly free of deleterious size effects, [27] which agrees well with the result of first-principles calculations. [35]  $h_c$  of SRO/BTO/SRO FTJ is about four BTO unit cells, which is consistent well with our previous results. [27] The qualitative result that  $h_c$  of Pt/BTO/Pt FTJ is smaller than that

of SRO/BTO/SRO FTJ in this work is consistent well with those of first-principles calculations [35] and lattice model. [57] However, our results are in contrast with previous works [31, 36, 37] predicting  $h_c$  of SRO/BTO/SRO FTJ to be smaller than that of Pt/BTO/Pt FTJ. In these previous works, [36, 37] Mehta *et al.*' electrostatic theory about the depolarizing field ( $\vec{E}_{dep} = -\frac{\vec{P}}{\varepsilon_b}(1 - \frac{h/\varepsilon_b}{l_{s1}/\varepsilon_{e1} + l_{s2}/\varepsilon_{e2} + h/\varepsilon_b})$ ) where  $l_{s1}$  and  $l_{s2}$  are Thomas-Fermi screening lengths and  $\varepsilon_{e1}$  and  $\varepsilon_{e2}$  are dielectric constants of electrode 1 and 2) is used [29] while in our work we used the "effective screening length" model to describe the depolarizing field (see Eq. (3)). Note that we used the same parameters as Refs. 36 and 37 except for the model of depolarizing field. [65] The distinct results are understandable since it is generally accepted that imperfect screening should be characterized by effective screening length (See Eq. (3)) rather than Thomas-Fermi one in Mehta *et al.*' model. [49] In fact, the effective screening length at Pt/BTO interface is only 0.03 Å [35] much smaller than that of Thomas-Fermi one  $\sim 0.4$  Å, [31] so a significantly reduced depolarizing field is expected and it would result in nearly no  $h_c$  in Pt/BTO/Pt FTJs. Previous study attributes this freedom of size effects in the Pt/BTO/Pt structure to the "negative dead layer" near the Pt/BTO interface, [35] while we argue that it may result directly from the fact that the effective screening length of Pt electrode is extremely small since Bratkovsky and Levanyuk suggested the "dead layer" model is totally equivalent as to consider an electrode with a finite screening length. [58] Here we ignore the effect of the extrinsic "dead layer" formed between metal electrode (i.e. Au or Pt) and a perovskite FE (i.e. Pb(ZrTi)O<sub>3</sub> or BTO). Indeed, Lou and Wang found that the "dead layer" between Pt and Pb(ZrTi)O<sub>3</sub> is extrinsic and could be removed almost completely by doping 2% Mn. [59] Experimentally, many researchers found that SRO/BTO/SRO capacitors (as well as other perovskite FE structures with conductive oxide electrodes) are free from passive layers. [31, 60, 61] Recently, a very interesting experimental result demonstrates that the RuO<sub>2</sub>/BaO terminations at BTO/SRO interface, which is assumed as many pinned interface dipoles and plays a detrimental role in stabilizing a switchable FE polarization, can be overcome by depositing a very thin layer of SrTiO<sub>3</sub> between BTO layer and SRO electrode. [41, 42] Nonetheless, it is still unclear whether such pinned interface dipoles are intrinsic and can be found in other FE/electrode interfaces (i.e. SRO/PbTiO<sub>3</sub> and Pt/BTO).

In the asymmetric structures in Fig. 3, it is shown that in comparison with  $\delta\varphi = 0$  in asymmetric Pt/BTO/SRO FTJs,  $h_c$  is significantly enhanced, as  $\delta\varphi$  increases, which is in good agreement with the recent results regarding  $\vec{E}_{bi}$  as short-range interface field, [41] and is similar with the previous results. [37] Note that  $\delta\varphi$  is intrinsic and determined strictly by the electronic and chemical envi-

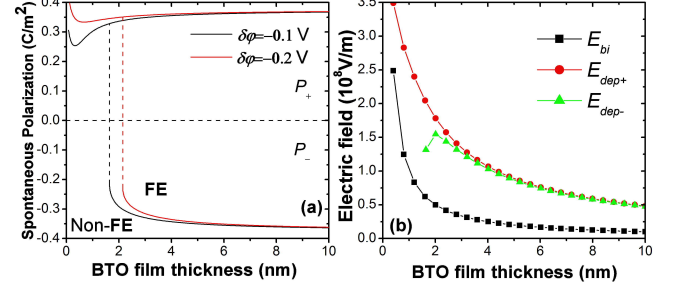


FIG. 4. (a): Polarization state  $P_{\pm}$  of the asymmetric Pt/BTO/SRO tunnel junctions as a function of BTO layer thickness with  $\delta\varphi = -0.1$  V and  $-0.2$  V in zero applied field at 0 K, respectively. The dash lines mark the boundary between polar non-FE and FE phases for different values of  $\delta\varphi$ ; (b): Dependence of the strengths of the built-in field  $E_{bi}$  and depolarizing field for different directions,  $E_{dep+}$  and  $E_{dep-}$  on the BTO layer thickness with  $\delta\varphi = -0.1$  V at 0 K.

ronments of FE/electrode interfaces but not by any potential drop through the FTJ which "creates" an applied field. [33, 34, 43, 44] Changing  $\delta\varphi$  is simply due to the lack of its exact value and for the purpose of studying the effect of  $\vec{E}_{bi}$  in asymmetric FTJs, which is similar to the previous method. [36, 37] This method [36, 37] indeed does not mean that any asymmetric electrodes are considered here, since the electrode is replaced, the electrode/FE interface parameters in Eqs. (1)-(3) such as  $\lambda_i$  and other interface parameters will also change. The variation of  $P_{+}$  in Pt/BTO/SRO FTJs as a function of the whole BTO layer thickness with  $\delta\varphi = -0.1$  V and  $-0.2$  V at 0 K is shown in Fig. 4(a). It is found that below the critical thickness  $P_{+}$  state shows an interesting recovery of a polar non-FE polarization, in contrast to  $P_{-}$  state (see Fig. 4(a)), becoming less significant when  $\delta\varphi \sim -0.2$  V. Note that such recovery has been reported in FE superlattices with asymmetric electrodes and demonstrated to be independent of the interfacial space charge. [46] Although such a recovery of polar non-FE polarization in BTO layer does not mean the recovery of ferroelectricity as it is not switchable, it is necessary to realize its origin. We plot the built-in field  $E_{bi}$  and depolarizing field for different directions,  $E_{dep+}$  and  $E_{dep-}$ , as a function of the BTO film thickness considering  $\delta\varphi = -0.1$  V as an example in Fig. 4(b). For the condition of  $P_{-}$  state as schematically illustrated in Fig. 1(b),  $E_{dep-}$  shows the typical behavior as the FTJ with the same electrodes, [30-32, 57] which means that  $E_{dep-}$  plays a key role forcing the single domain in the FE layer to destabilize as the film thickness is decreased.  $E_{bi}$  with the same direction of  $E_{dep-}$  helps then to speed up such destabi-

lization, therefore enhancing the critical thickness. For the  $P_+$  state,  $E_{dep+}$  and  $E_{bi}$  are in the opposite directions, as depicted in Fig. 1(a), and both the strengths of  $E_{dep+}$  and  $E_{bi}$  increase as the BTO layer thickness is decreased (Fig. 4(b)), which means that  $E_{dep+}$  is partially cancelled by  $E_{bi}$ . The strength of this partial compensation becomes stronger with the film thickness decreasing (see the slopes of  $E_{bi}-h$  and  $E_{dep+}-h$  curves)(Fig. 4(b)). Therefore,  $E_{bi}$  is fighting against  $E_{dep+}$  allowing the polarization to recover into a polar non-FE polarization. This recovery of polar non-FE polarization forces the system to a higher energy state which strongly supports our forgoing predictions of local rotations of non-switchable polarization ( $<90^\circ$ ) and the formation of closure-like domain structure to minimize the system energy.

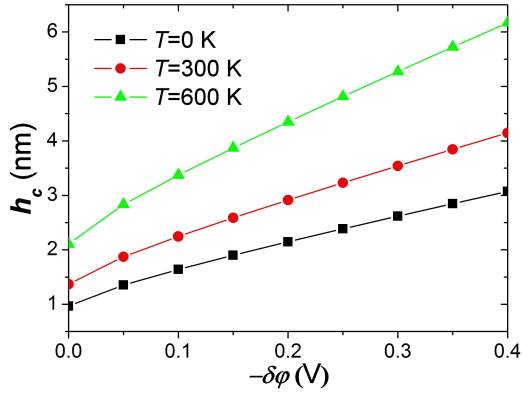


FIG. 5. The variation in critical thickness  $h_c$  in epitaxial asymmetric Pt/BTO/SRO tunnel junctions as a function of  $-\delta\varphi$  at three different temperatures: 0 K, 300 K, and 600 K, respectively ( $E=0$  kV/cm).

The critical thickness  $h_c$  under different ambient temperatures  $T$  as a function of  $(-\delta\varphi)$  in asymmetric Pt/BTO/SRO FTJs is shown in Fig. 5. It can be seen that  $h_c$  decreases with  $T$  increasing. And it is found that for other  $T$ , the asymmetric Pt/BTO/SRO FTJs show a similar behavior of enhancement of  $h_c$  by increasing the strength of  $\vec{E}_{bi}$  as shown in Fig. 3 at 0 K.

### Transition temperature and dielectric response

The transition temperature  $T_c$  of the asymmetric FTJs is extremely important, especially for the device applications. Fig. 6 summarizes  $T_c$  as a function of BTO thickness in epitaxial asymmetric Pt/BTO/SRO FTJs at various values of  $\delta\varphi$ . It is shown that  $T_c$  in asymmetric Pt/BTO/SRO FTJs monotonically decreases with the BTO layer thickness decreasing, which is similar to the behavior of symmetric SRO/BTO/SRO or Pt/BTO/Pt FTJs. [27] Moreover,  $T_c$  decreases more significantly for

thinner BTO barrier layer thickness (see the slope of  $T_c-h$  curves in Fig. 6). At a given BTO layer thickness, it is found in Fig. 7 that  $T_c$  decreases as  $\delta\varphi$  becomes more negative, which means a larger built-in field can force the phase transition to occur at lower temperatures. The transition temperature  $T_c$  is strongly sensitive to the  $\delta\varphi$  change especially for the thinner BTO barrier (see the slope of  $T_c-(-\delta\varphi)$  curves in Fig. 7). It can be clearly seen that the FE transition temperature is suppressed as the built-in field is increased for different BTO thicknesses. Usually, the TER effect is always significantly larger for thicker barrier with larger polarization. [3, 5] Here we find that a fundamental limit (which is more drastic for thinner FE barrier thickness) on the work temperature of FTJ-type or capacitor-type devices should also be simultaneously taken into account together with the FE barrier thickness or polarization value. In addition and interestingly, since the electrocaloric effect is always the strongest close to the FE-PE transition, [62] such tuning of  $T_c$  by  $\vec{E}_{bi}$  should be also considered in potential asymmetric FTJs for the room temperature solid-state refrigeration. [27] Moreover, the fact that large tunneling current in asymmetric FTJs [6] results in significant Joule heating should also be included in the design of future devices.

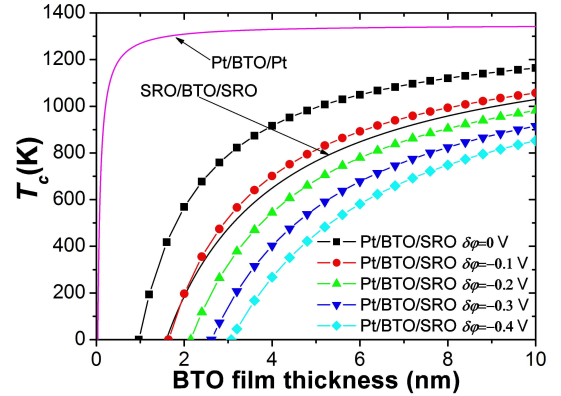


FIG. 6. The transition temperature  $T_c$  as a function of BTO layer thickness in epitaxial asymmetric Pt/BTO/SRO tunnel junctions at various values of  $\delta\varphi$  with no applied field. The results of symmetric SRO/BTO/SRO and Pt/BTO/Pt tunnel junctions [27] are also provided for comparison.

The dielectric response  $\varepsilon_+$  ( $\vec{E}$  is parallel to  $\vec{E}_{bi}$ ) and  $\varepsilon_-$  ( $\vec{E}$  is antiparallel to  $\vec{E}_{bi}$ ) of Pt/BTO/SRO FTJs (consider the 5-nm-thick BTO film as an example) as a function of  $T$  at different  $\delta\varphi$  is shown in Figs. 8(a) and (b). Several key parameters with different  $\delta\varphi$  in Fig. 8(a) are extracted in Table. I:  $T_{max}$  corresponds to the temperature where  $\varepsilon_+$  reaches its maximum,  $\varepsilon_{max+}$ ;  $\varepsilon_{min+}$  simply means the minimal value of  $\varepsilon_+$ ;  $\delta\varepsilon_d$  is somehow the diffuseness of the transition. It can be seen that when

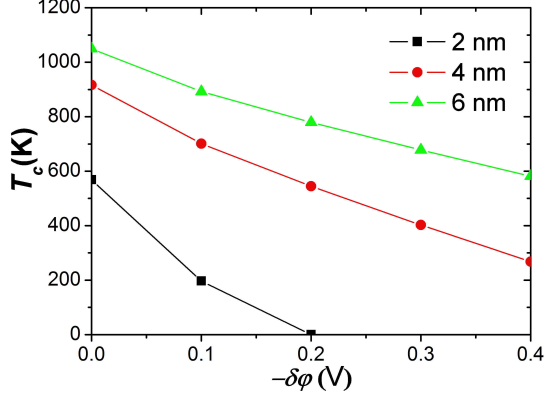


FIG. 7. The transition temperature  $T_c$  as a function of  $(-\delta\varphi)$  in epitaxial asymmetric Pt/BTO/SRO tunnel junctions with three different BTO layer thicknesses: 2 nm, 4 nm and 6 nm, respectively ( $E=0$  kV/cm).

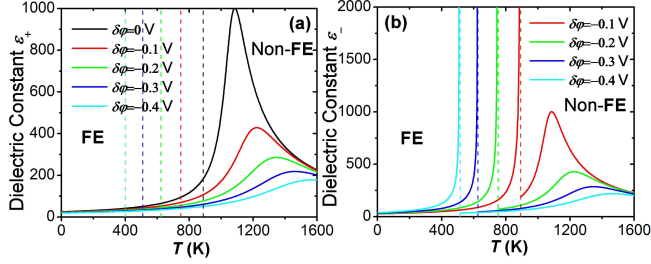


FIG. 8. Dielectric constants  $\epsilon_+$  (a) and  $\epsilon_-$  (b) as a function of temperature  $T$  at various values of  $\delta\varphi$  in asymmetric Pt/BTO/SRO tunnel junctions where BTO layer thickness  $h$  is 5 nm ( $E=100$  kV/cm). The dash lines mark the boundary between polar non-FE and FE phases for different values of  $\delta\varphi$ .

$\delta\varphi = 0$ ,  $\epsilon_+$  shows a sharp peak near  $T_c$ . However, a gradual decrease in  $\epsilon_{max}$  and  $\delta\epsilon_d$  is seen upon increasing  $\epsilon_+$  which is well consistent with the results of smearing of  $T_c$  by increasing  $\epsilon_+$  in Fig. 6 (see the slope of  $T_c - h$  curves in Fig. 6). The diffusive transition response in  $\epsilon_+$  clearly shows smearing of the phase transition as a result of  $\vec{E}_{bi}$ , which verifies the predictions of Tagantsev *et al* [33, 34] and Bratkovsky *et al.* [44] In addition, it is shown  $T_{max}$  is shifted to higher temperatures due to  $\vec{E}_{bi}$ . As the strength of  $\vec{E}_{bi}$  increases, the smearing of phase transition and the shift of  $T_{max}$  becomes more significant. On the other hand, the applied field cannot fully compensate the built-in field, resulting in a discontin-

TABLE I. The different parameters extracted from Fig. 8(a).

$\delta\varphi$ (V)	$T_{max}$ (K)	$\epsilon_{max+}$	$\epsilon_{min+}$	$\delta\epsilon_d = (\epsilon_{max+} - \epsilon_{min+})/2$
0	1086	1001.4	24.8	513.1
-0.1	1223	428.5	23.0	225.7
-0.2	1345	285.8	21.4	153.6
-0.3	1465	218.3	20.1	119.2
-0.4	1574	178.1	18.9	98.5

uous phase transition from FE phase to polar non-FE phase with temperature increasing as depicted in dielectric response  $\epsilon_-$  in Fig. 8(b), which is distinct from the continuous counterpart of  $\epsilon_+$  as shown in Fig. 8(a).  $P_-$  abruptly changes its sign near the transition point resulting a dielectric peak and a similar smearing of  $\epsilon_-$  by increasing the strength of  $\vec{E}_{bi}$  is found. Furthermore, it is found that though the transition temperatures for two directions are different, they both decrease as the built-in field increases which is consistent with the results without any external field (See Fig. 6), which indicates that the built-in field forces the transition to take place at a reduced temperature.

### Comments on the built-in field effect

We make further comments on the built-in field effect in asymmetric FTJs. The main assumption in this study is that  $\delta\varphi$  does not change during the polarization reversal. [33, 34] The presence of  $\delta\varphi$  which results in an asymmetric potential energy and barrier height differences by switching the polarization will induce the TER effect. [1–3] Note that the switching of the polarization in the asymmetric FTJs may change the value of  $\delta\varphi$ . [4, 18, 40, 63, 64] However, according to our analysis, the variation in  $\delta\varphi$  (even changing its sign occurs during the polarization reversal) does not alter the main results of this study due to its induced broken spatial inversion symmetry of FTJs. In addition to the built-in field, if the surface term  $\delta\zeta = (\zeta_2 - \zeta_1)$  is nonzero, the main conclusions of this paper will not change as well.

### CONCLUSIONS

In summary, on the basis of a multiscale thermodynamic model, a detailed analysis of the changes brought by the built-in electric field in asymmetric FTJs is made. It is demonstrated that the critical thickness does exist in asymmetric FTJs. Below the critical thickness, it is found that there is a recovery of polar non-FE polarization due to strong cancelling of the depolarizing field by the built-in field, and closure-like domains are proposed

to form to minimize the system energy. It is found that the built-in electric field could not only induce imprint and a behavior of smearing of the FE phase transition but also forces the phase transition to take place at a reduced temperature. A fundamental limit of transition temperature dependence of the barrier layer thickness on the work temperature of FTJ-type or FE capacitor-type devices is proposed and should be simultaneously taken into account in the further experiments. Hopefully, our results will be helpful to the fundamental understandings of phase transitions in asymmetric FTJs.

This work is supported by the Ministry of Science and Technology of China through a 973-Project under Grant No. 2012CB619401. The authors gratefully thank Dr. X. Y. Wang, Dr. M. B. Okatan, and Prof. S. P. Alpay for their fruitful suggestions. Y. Liu is thankful to the Multidisciplinary Materials Research Center (MMRC) at Xi'an Jiaotong University for hospitality during his visit. Y. Liu and B. Dkhil wish to thank the China Scholarship Council (CSC) for funding YL's stay in France. Y. Liu, M. Bibes and B. Dkhil also acknowledge the Agence Nationale pour la Recherche for financial support through NOMILOPS (ANR-11-BS10-016-02) project. X. J. Lou would like to thank the "One Thousand Youth Talents" program for support.

---

\* liuyangphy52@gmail.com

- [1] E. Y. Tsymbal, A. Gruverman, V. Garcia, M. Bibes, and A. Barthélemy, *MRS Bulletin* **37**, 138 (2012).
- [2] H. Kohlstedt, N. A. Pertsev, J. Rodríguez Contreras, and R. Waser, *Phys. Rev. B* **72**, 125341 (2005).
- [3] M. Y. Zhuravlev, R. F. Sabirianov, S. S. Jaswal, and E. Y. Tsymbal, *Phys. Rev. Lett.* **94**, 246802 (2005).
- [4] J. P. Velev, C.-G. Duan, K. D. Belashchenko, S. S. Jaswal, and E. Y. Tsymbal, *Phys. Rev. Lett.* **98**, 137201 (2007).
- [5] V. Garcia, S. Fusil, K. Bouzehouane, S. Enouz-Vedrenne, N. D. Mathur, A. Barthélemy, and M. Bibes, *Nature (London)* **460**, 81 (2009).
- [6] A. Gruverman, D. Wu, H. Lu, Y. Wang, H. W. Jang, C. M. Folkman, M. Y. Zhuravlev, D. Felker, M. Rzechowski, C. B. Eom, and E. Y. Tsymbal, *Nano Lett.* **9**, 3539 (2009).
- [7] A. Crassous, V. Garcia, K. Bouzehouane, S. Fusil, A. H. G. Vlooswijk, G. Rispens, B. Noheda, M. Bibes, and A. Barthélemy, *Appl. Phys. Lett.* **96**, 042901 (2010).
- [8] A. Chanthbouala, A. Crassous, V. Garcia, K. Bouzehouane, S. Fusil, X. Moya, J. Allibe, B. Dlubak, J. Grollier, S. Xavier, C. Deranlot, A. Moshar, R. Proksch, N. D. Mathur, M. Bibes, and A. Barthélemy, *Nat. Nanotechnol.* **7**, 101 (2011).
- [9] D. I. Bilc, F. D. Novaes, J. Íñiguez, P. Ordejón, and P. Ghosez, *ACS Nano* **6**(2), 1473 (2012).
- [10] D. Pantel, H. D. Lu, S. Goetze, P. Werner, D. J. Kim, A. Gruverman, D. Hesse, and M. Alexe, *Appl. Phys. Lett.* **100**, 232902 (2012).
- [11] A. Chanthbouala, V. Garcia, R. O. Cherifi, K. Bouzehouane, S. Fusil, X. Moya, S. Xavier, H. Yamada, C. Deranlot, N. D. Mathur, M. Bibes, A. Barthélemy, and J. Grollier, *Nat. Mater.* **11**, 860 (2012).
- [12] M. Y. Zhuravlev, S. S. Jaswal, E. Y. Tsymbal, and R. F. Sabirianov, *Appl. Phys. Lett.* **87**, 222114 (2005).
- [13] C.-G. Duan, S. S. Jaswal, and E. Y. Tsymbal, *Phys. Rev. Lett.* **97**, 047201 (2006).
- [14] S. Sahoo, S. Polisetty, C.-G. Duan, S. S. Jaswal, E. Y. Tsymbal, and C. Binek, *Phys. Rev. B* **76**, 092108 (2007).
- [15] C.-G. Duan, Julian P. Velev, R. F. Sabirianov, W. N. Mei, S. S. Jaswal, and E. Y. Tsymbal, *Appl. Phys. Lett.* **92**, 122905 (2008).
- [16] M. K. Niranjan, J. D. Burton, J. P. Velev, S. S. Jaswal, and E. Y. Tsymbal, *Appl. Phys. Lett.* **95**, 052501 (2009).
- [17] J. D. Burton and E. Y. Tsymbal, *Phys. Rev. B* **80**, 174406 (2009).
- [18] J. P. Velev, C.-G. Duan, J. D. Burton, A. Smogunov, M. K. Niranjan, E. Tosatti, S. S. Jaswal, and E. Y. Tsymbal, *Nano Lett.* **9**, 427 (2009).
- [19] M. Y. Zhuravlev, S. Maekawa, and E. Y. Tsymbal, *Phys. Rev. B* **81**, 104419 (2010).
- [20] V. Garcia, M. Bibes, L. Bocher, S. Valencia, F. Kronast, A. Crassous, X. Moya, S. Enouz-Vedrenne, A. Gloter, D. Imhoff, C. Deranlot, N. D. Mathur, S. Fusil, K. Bouzehouane, and A. Barthélemy, *Science* **327**, 1106 (2010).
- [21] M. Hambe, A. Petraru, N. A. Pertsev, P. Munroe, V. Nagarajan, and H. Kohlstedt, *Adv. Funct. Mater.* **20**, 2436 (2010).
- [22] S. Valencia, A. Crassous, L. Bocher, V. Garcia, X. Moya, R. O. Cherifi, C. Deranlot, K. Bouzehouane, S. Fusil, A. Zobel, A. Gloter, N. D. Mathur, A. Gaupp, R. Abrudan, F. Radu, A. Barthélemy, and M. Bibes, *Nat. Mater.* **10**, 753 (2011).
- [23] H. L. Meyerheim, F. Klimenta, A. Ernst, K. Mohseni, S. Ostanin, M. Fechner, S. Parihar, I. V. Maznichenko, I. Mertig, and J. Kirschner, *Phys. Rev. Lett.* **106**, 087203 (2011).
- [24] L. Bocher, A. Gloter, A. Crassous, V. Garcia, K. March, A. Zobel, S. Valencia, S. Enouz-Vedrenne, X. Moya, N. D. Mathur, C. Deranlot, S. Fusil, K. Bouzehouane, M. Bibes, A. Barthélemy, C. Colliex, and O. Stáphan, *Nano Lett.* **12**, 376 (2012).
- [25] J. M. López-Encarnación, J. D. Burton, Evgeny Y. Tsymbal, and J. P. Velev, *Nano Lett.* **11**, 599 (2011).
- [26] D. Pantel, S. Goetze, D. Hesse, and M. Alexe, *Nat. Mater.* **11**, 289 (2012).
- [27] Y. Liu, X.-P. Peng, X. J. Lou, and H. Zhou, *Appl. Phys. Lett.* **100**, 192902 (2012).
- [28] X. Luo, B. Wang, and Y. Zheng, *ACS Nano* **5**(3), 1649 (2011); H. Lu, D. J. Kim, C.-W. Bark, S. Ryu, C. B. Eom, E. Y. Tsymbal, and A. Gruverman, *Nano Lett.* **12**, 6289 (2012).
- [29] R. R. Mehta, B. D. Silverman, and J. T. Jacobs, *J. Appl. Phys.* **44**, 3379 (1973).
- [30] J. Junquera and P. Ghosez, *Nature (London)* **422**, 506 (2003).
- [31] D. J. Kim, J. Y. Jo, Y. S. Kim, Y. J. Chang, J. S. Lee, J.-G. Yoon, T. K. Song, and T. W. Noh, *Phys. Rev. Lett.* **95**, 237602 (2005).
- [32] N. A. Pertsev and H. Kohlstedt, *Phys. Rev. Lett.* **98**, 257603 (2007).
- [33] G. Gerra, A. K. Tagantsev, and N. Setter, *Phys. Rev. Lett.* **98**, 207601 (2007).

- [34] A. K. Tagantsev, G. Gerra, and N. Setter, *Phys. Rev. B* **77**, 174111 (2008).
- [35] M. Stengel, D. Vanderbilt, and N. A. Spaldin, *Nature Mater.* **8**, 392 (2009).
- [36] Y. Zheng, W. J. Chen, C. H. Woo, and B. Wang, *J. Phys. D: Appl. Phys.* **44**, 139501 (2011).
- [37] Y. Zheng, W. J. Chen, X. Luo, B. Wang, and C. H. Woo, *Acta Materialia* **44**, 139501 (2012).
- [38] M.-Q. Cai, Y. Zheng, P.-W. Ma, and C. H. Woo, *J. Appl. Phys.* **109**, 024103 (2011).
- [39] M.-Q. Cai, Y. Du, and B.-Y. Huang, *Appl. Phys. Lett.* **98**, 102907 (2011).
- [40] Y. Umeno, J. M. Albina, B. Meyer, and C. Elsässer, *Phys. Rev. B* **80**, 205122 (2009).
- [41] X. H. Liu, Y. Wang, P. V. Lukashev, J. D. Burton, and E. Y. Tsymbal, *Phys. Rev. B* **85**, 125407 (2012).
- [42] H. Lu, X. Liu, J. D. Burton, C.-W. Bark, Y. Wang, Y. Zhang, D. J. Kim, A. Stamm, P. Lukashev, D. A. Felker, C. M. Folkman, P. Gao, M. S. Rzchowski, X. Q. Pan, C.-B. Eom, E. Y. Tsymbal, and A. Gruverman, *Adv. Mater.* **24**, 1209 (2012).
- [43] J. G. Simmons, *Phys. Rev. Lett.* **10**, 10 (1963).
- [44] A. M. Bratkovsky and A. P. Levanyuk, *Phys. Rev. Lett.* **94**, 107601 (2005).
- [45] J. F. Scott, *Ferroelectric Memories* (Springer, Berlin, 2000).
- [46] Y. Liu and X.-P. Peng, *Applied Physics Express* **5**, 011501 (2012).
- [47] Y. Liu and X.-P. Peng, *Chinese Physics Letters* **29**, 057701 (2012).
- [48] M. B. Okatan, I. B. Misirlioglu, and S. P. Alpay, *Phys. Rev. B* **82**, 094115 (2010).
- [49] J. Junquera and P. Ghosez, *J. Comput. Theor. Nanosci.* **5**, 2071 (2008).
- [50] I. I. Naumov, L. Bellaiche, and H. X. Fu, *Nature (London)* **432**, 737 (2004).
- [51] I. Naumov and A. M. Bratkovsky, *Phys. Rev. Lett.* **101**, 107601 (2008).
- [52] I. Kornev, H. X. Fu, and L. Bellaiche, *Phys. Rev. Lett.* **93**, 196104 (2004).
- [53] P. Aguado-Puente and J. Junquera, *Phys. Rev. Lett.* **100**, 177601 (2008).
- [54] T. Shimada, S. Tomoda, and T. Kitamura, *Phys. Rev. B* **81**, 144116 (2010).
- [55] C. T. Nelson, B. Winchester, Y. Zhang, S.-J. Kim, A. Melville, C. Adamo, C. M. Folkman, S.-H. Baek, C.-B. Eom, D. G. Schlom, L.-Q. Chen, and X. Q. Pan, *Nano Lett.* **11**, 828 (2011).
- [56] C.-L. Jia, K. W. Urban, M. Alexe, D. Hesse, and I. Vrejoiu, *Science* **331**, 1420 (2011).
- [57] X. Y. Wang, Y. L. Wang, and R. J. Yang, *Appl. Phys. Lett.* **95**, 142910 (2009); Y. L. Wang, X. Y. Wang, Y. Liu, B. T. Liu, and G. S. Fu, *Physics Letters A*, **374**, 4915 (2010).
- [58] A. M. Bratkovsky and A. P. Levanyuk, *J. Comp. Theor. Nanosci.* **6**, 465 (2005).
- [59] X. J. Lou and J. Wang, *Journal of Physics: Condensed Matter* **22**, 055901 (2010).
- [60] Y. S. Kim, J. Y. Jo, D. J. Kim, Y. J. Chang, J. H. Lee, T. W. Noh, T. K. Songa, J.-G. Yoon, J.-S. Chung, S. I. Baik, Y.-W. Kim, and C. U. Jung, *Appl. Phys. Lett.* **88**, 072909 (2006).
- [61] H. Z. Jin and J. Zhu, *J. Appl. Phys.* **92**, 4594 (2002).
- [62] J. F. Scott, *Annu. Rev. Mater. Res.* **41**, 229 (2011).
- [63] M. Stengel, P. Aguado-Puente, N. A. Spaldin, and J. Junquera, *Phys. Rev. B* **83**, 235112 (2011).
- [64] F. Chen and A. Klein, *Phys. Rev. B* **86**, 094105 (2012).
- [65] We used the following set of parameters (in SI units):  $u_m = -0.02458$ ,  $Q_{12} = -0.045$ ,  $\epsilon_0 = 8.85 \times 10^{-12}$ ,  $\epsilon_b \approx 50\epsilon_0$ ,  $S_{11} = 8.3 \times 10^{-12}$ ,  $S_{12} = -2.7 \times 10^{-12}$ ,  $\eta_{SRO} = 0.113$ ,  $\eta_{Pt} = 0.113$ ,  $\lambda_{SRO} = 1.2 \times 10^{-11}$ ,  $\lambda_{Pt} = 3 \times 10^{-13}$ . Landau coefficients  $\alpha_i^*$  (the expressions can be originally found in N. A. Pertsev, A. K. Tagantsev, and N. Setter, *Phys. Rev. B* **61**, R825 (2000)), electrostrictive coefficients, and elastic compliances of BTO at room temperature we used are the same as those in Refs. 27, 36 and 37. The effective screening length  $\lambda_i$  and the coefficients of the surface energy expansion  $\eta_i$  are taken from Refs. 33, 34 and 35, respectively. The background dielectric constant  $\epsilon_b$  is taken from Refs. 36 and 37 which is distinct from  $7\epsilon_0$  used in Refs. 33 and 34. In fact, there is no consensus on its exact value, especially by the theoretical researchers. In this study, we have made some comparisons with the previous studies in Refs. 36 and 37, so selecting  $50\epsilon_0$  is reasonable and does not change the main results of this work. The approximated parameters in this work need more rigorous treatment by the first-principles calculations or experimental confirmation in the future.